EXPERIMENTAL INVESTIGATIONS ON THE ICE-FORMING ABILITY OF VARIOUS CHEMICAL SUBSTANCES

By Norihiko Fukuta

Chemical Institute, Nagoya University, Nagoya, Japan

(Original manuscript received 29 April 1957; revised manuscript received 12 June 1957)

ABSTRACT

A careful survey of the methods for measuring ice nucleation was made. Errors of previous investigations based on the relationship between the time lag of ice formation and the falling velocity of ice particles through a temperature gradient zone were avoided. Experiments were made on a large number of chemicals by using a thermostat-type cloud chamber, the threshold temperatures for ice nucleation of these chemicals were determined precisely and found to be somewhat higher than those of previous workers. Analysis of the experimental data shows the following: 1. the highly effective nuclei are all insoluble in water; 2. particles with the greatest structural similarity to ice make the most effective nuclei; 3. the stronger the ionic nature of nuclei crystals, the more effective are they as ice nuclei. These latter two factors are mutually interdependent. An explanation of the mechanism of ice formation is presented.

1. Introduction

A most interesting, yet highly complicated phenomena is the transformation of supercooled clouds into ice crystals by small particles of smoke. Since Vonnegut [1] first discovered the effectiveness of silver iodide as an ice crystal nucleus, considerable theoretical and experimental work on ice nucleation has been reported by various workers in the field of experimental meteorology. The three sorts of cloud chambers which have been employed are the so-called Wilson cloud chamber, the continuous cloud chamber, and the thermostat-type cloud chamber, to determine the threshold temperatures at which ice nucleation begins for many kinds of chemicals.

The method used in the Wilson cloud chamber for ice nucleation is the rapid expansion of the air containing moisture to produce a supercooled water cloud without a temperature gradient and to observe the behavior of various ice nuclei. Cwilong [2] early used this type of small table-model expansion chamber, and later Fournier d'Albe [3] also employed the same type of apparatus. More recently Mossop [4; 5] has used the Wilson cloud chamber, and discussed the dependence of ice-forming ability on the structural similarity of ice-forming nuclei to ice crystals.

Schaefer [6] devised another very convenient chamber which has been called a continuous cloud chamber. The walls and the bottom of the chamber are cooled by dry ice, moisture is supplied from an upper reservoir and there is a stable temperature gradient so that the threshold temperatures of added and then gradually sedimenting nuclei can be determined in the uppermost zone where ice nucleation begins. By using this chamber, Hosler [7] observed threshold temperatures of a number of water-soluble salts, insoluble salts and gases. Asada [8] tested the activities of various substances of cubic and hexagonal shape considered similar to ice structure and consequently discovered the effectiveness of aluminum oxide. Sano and his co-workers [9] in this laboratory recently investigated the ice-forming ability of a large number of compounds and discovered the effectiveness of nickel oxide as an ice nucleus.

Prior to this author's work, there were few investigators who used the thermostat-type cloud chamber without a temperature gradient. H. aufm Kampe [10] discovered the effectiveness of natural and artificial aerosols—AgI ($-3 \sim -5C$), CdI_2 and CoI_2—in a chamber of this type. Birstein [11] examined the ice-forming abilities of various smokes at -20C, produced in an atmosphere of nitrogen, and pointed out the difference in ice-forming abilities between smokes produced in air and those formed under a nitrogen atmosphere.

There is some disagreement in the data described in the above papers, however, because it is not always possible to reproduce a smoke of particles which have the same size distribution, the same surface properties and the same atmospheric conditions. Consequently, with such disagreement, it is not possible to solve the problems pertaining to the mechanisms of atmospheric phase transition.

It is clear that the method of the continuous cloud chamber contains a few sources of error; therefore, in order to avoid these difficulties, a new thermostat-type cloud chamber was devised and the threshold temperatures of a large number of chemicals were measured by using the chamber in the temperature range between $0 \sim -20$C; results differing somewhat from those of previous investigators were obtained.

2. Experimental

Preparation of samples.—Samples used in this experiment were prepared by the author or purchased from chemical houses. The methods of preparation of samples are shown in a condensed form as follows:

1.	LiF	$Li_2CO_3(EP) + HCl(GP) \longrightarrow LiCl$ $LiCl + KF \longrightarrow LiF$	(12)
2.	NaBr	$NaOH(GP) + HBr(GP) \longrightarrow NaBr$	(12)
3.	CuF_2	$CuSO_4(EP, recryst.) + KF(EP) \longrightarrow CuF_2$	
4.	Cu_2Cl_2	$CuSO_4(EP, recryst.) + NaOH(EP) \longrightarrow NaCu(OH)_2$ $NaCu(OH)_2 + HCl + Cu \xrightarrow{diluted} Cu_2Cl_2$	
5.	Cu_2Br_2	$CuSO_4(EP, recryst.) + KBr(GP) + Cu \longrightarrow Cu_2Br_2$	(12)
6.	Cu_2I_2	$CuSO_4(EP) + KI(GP) + FeSO_4(EP) \longrightarrow Cu_2I_2$	(12)
7.	Cu_2O	$CuSO_4(EP, recryst.) + NaOH(EP) \longrightarrow Cu(OH)_2$ $Cu(OH)_2 + NH_4OH + glucose \xrightarrow{boiled} Cu_2O$	
8.	CuO	$CuSO_4(EP, recryst.) + NaOH(EP) \longrightarrow Cu(OH)_2$ $Cu(OH)_2 \xrightarrow{heated} CuO$	(12)
9.	CuS	$CuSO_4(EP, recryst.) + Na_2S(GP) \longrightarrow CuS$	
10.	AgCl	$AgNO_3(GP) + KCl(GP) \longrightarrow AgCl$	(12)
11.	AgBr	$AgNO_3(GP) + KBr(GP) \longrightarrow AgBr$	(12)
12.	AgI	$AgNO_3(GP) + KI(GP) \longrightarrow AgI$	(13)
13.	Ag_2O	$AgNO_3(GP) + NaOH(EP) \xrightarrow{boiled} Ag_2O$	(13)
14.	Ag_2S	$AgNO_3(GP) + Na_2S(GP) \longrightarrow Ag_2S$	
15.	CaF_2	$CaCO_3(GP) + HF(EP) \longrightarrow CaF_2$	(13)
16.	$CaI_2 \cdot 6H_2O$	$CaCO_3(GP) + HI(GP) \xrightarrow{dried\ up} CaI_2 \cdot 6H_2O$	
17.	BaF_2	$BaCl_2(CP) + HF(EP) \longrightarrow BaF_2$	
18.	MgF_2	$MgCl_2(CP) + HF(EP) \longrightarrow MgF_2$	
19.	$MgBr_2 \cdot 6H_2O$	$MgO(EP) + HBr(GP) \xrightarrow{dried\ up} MgBr_2 \cdot 6H_2O$	(12)
20.	MgO	$Mg(EP) + O_2 \xrightarrow{heated} MgO$	
21.	MgTe	$Mg(EP) + Te\ (sublimed\ in\ vacuum) \xrightarrow{heated\ in\ H_2} MgTe$	(13)
22.	ZnF_2	$Zn(NO_3)_2(EP) + KF(EP) \longrightarrow ZnF_2$	
23.	ZnS	$Zn(NO_3)_2(CP) + Na_2S(GP) \xrightarrow{in\ acetic\ acid} ZnS$	
24.	CdF_2	$Cd(NO_3)_2(EP) + KF(EP) \longrightarrow CdF_2$	
25.	Hg_2Cl_2	$Hg_2(NO_3)_2(GP) + KCl(GP) \longrightarrow Hg_2Cl_2$	(12)
26.	Hg_2Br_2	$Hg_2(NO_3)_2(GP) + KBr(GP) \longrightarrow Hg_2Br_2$	(12)
27.	$HgBr_2$	$Hg(NO_3)_2(EP) + KBr(GP) \longrightarrow HgBr_2$	(12)
28.	Hg_2I_2	$Hg_2(NO_3)_2(GP) + KI(GP) \longrightarrow Hg_2I_2$	(12)
29.	HgO	$HgCl_2(GP) + cold\ NaOH(EP) \longrightarrow HgO$	(12)
30.	HgS	$HgCl_2(EP) + Na_2S(GP) \xrightarrow{in\ HNO_3} HgS$	(12)
31.	Al_2O_3	$Al(OH)_3 \xrightarrow{heated\ at\ 1300C} Al_2O_3$	(12)
32.	CeF_3	$Ce_2(CO_3)_2(CP) + HF(EP) \longrightarrow 2CeF_3 \cdot H_2O$ $2CeF_3 \cdot H_2O \xrightarrow{ignited} CeF_3$	(12)

33.	SnI_2	$SnCl_2(GP) + KI(GP) \longrightarrow SnI_2$	(13)
34.	SnO	$SnCl_2(GP) + NaOH(EP) \xrightarrow{\text{boiled}} SnO$	(12)
35.	SnO_2	$SnCl_4(CP) + NaOH(EP) \longrightarrow Sn(OH)_4$ $Sn(OH)_4 \xrightarrow{\text{ignited}} SnO_2$	
36.	SnS	$SnCl_2(GP) + H_2S \longrightarrow SnS$	(12)
37.	SnS_2	$SnCl_4(CP) + H_2S \longrightarrow SnS_2$	(12)
38.	PbF_2	$Pb(NO_3)_2(EP) + HF(EP) \longrightarrow PbF_2$	(12)
39.	$PbCl_2$	$Pb(NO_3)_2(Ag\text{-free}) + KCl(GP) \longrightarrow PbCl_2$	(12)
40.	$PbBr_2$	$Pb(NO_3)_2(Ag\text{-free}) + KBr(GP) \longrightarrow PbBr_2$	(12)
41.	PbI_2	$Pb(NO_3)_2(Ag\text{-free}) + KI(GP) \longrightarrow PbI_2$	(12)
42.	PbS	$Pb(NO_3)_2(Ag\text{-free}) + Na_2S(GP) \longrightarrow PbS$	(12)
43.	BiI_3	$Bi(NO_3)_3(GP) + KI(GP) \xrightarrow{\text{in acetic acid}} BiI_3$	(12)
44.	FeF_2	$FeSO_4(EP) + KF(EP) \longrightarrow FeF_2$	
45.	NiF_2	$NiCO_3(EP) + HF(EP) \longrightarrow NiF_2$	
46.	$NiBr_2$	$NiCO_3(EP) + HBr(GP) \longrightarrow NiBr_2$	
47.	NiO	$NiCO_3(EP) \xrightarrow{\text{ignited at 450C}} NiO$	(13)
48.	NiS	$Ni(NO_3)_2(EP) + H_2S \xrightarrow{\text{in acetic acid}} NiS$	(12)
49.	CoO	$CoCO_3(EP) \xrightarrow{\text{heated in vacuum at 800C}} CoO$	(13)
50.	CoS	$Co(NO_3)_2(EP) + Na_2S(EP) \longrightarrow CoS$	(12)

(No special reference represents reaction in aqueous solution. GP; guaranteed pure reagent, EP; extra pure reagent, CP; chemically pure reagent).

Smoke was generated by the dispersion method or the condensation method. The former is a convenient means of dispersing substances which have a low vapor pressure or are easily decomposed by heat. The dried powder blown into a smoke chamber is readily dispersed and gradually sediments; particles with a radius of 0.3 to 1.0 μ are easily selected. Particles thus obtained are considered to have the same crystalline structures as the original powders. The condensation method is usually used to disperse substances which are easily soluble in water or have low melting points. The sample is put into a porcelain boat or a crucible, heated, vaporized, and then cooled suddenly by mixing with air. The particles of smoke thus produced generally have radii in the range 0.05 to 0.4 μ. As has already been found [1; 9], the activity of particles for nucleation decreases considerably when the size is less than 0.1 μ in radius; therefore the larger particles made by cooling the vapor slowly were used in the experiment. For example, the particle size distribution of lead iodide smoke, produced by the condensation method and measured ultra-microscopically, is illustrated in fig. 1; it can be seen from the figure that there is a maximum frequency at about 0.2 μ radius.

Apparatus and procedure.—The apparatus used in this experiment is shown in fig. 2. In the figure, a glass-vessel (V_1) constructed of glass plates, of the dimensions 35 cm deep and 15 cm square, is dipped into a 25 per cent solution of calcium chloride (M) contained in a large glass vessel (V_2) surrounded by a thermally insulated box (I), the distance from the level of the solution to the upper surface of the lead block (Pb) is 22 cm. A concentrated aqueous solution

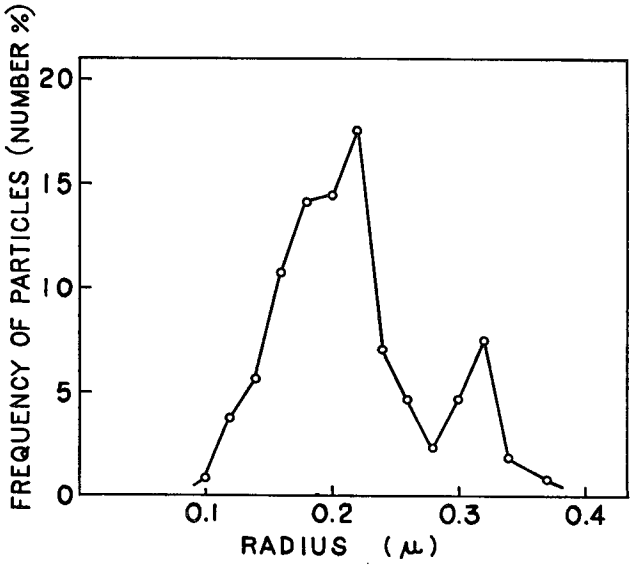

FIG. 1. Size distribution of lead iodide nuclei.

of calcium chloride, cooled by means of a refrigerator making use of fleon 12 (F) and of an expansior (E) and provided with a temperature regulating device (R), is maintained at a desired temperature within ±0.1C. Water vapor is supplied from a generator attached outside of an inlet (W). In order to measure the temperature of fog produced in the vessel, a copper-constantan thermocouple (T) is inserted, the induced thermo-electromotive force is then measured with the accuracy of one microvolt by means of a low-voltage potentiometer.

Fig. 3 is a graphic illustration of the relationship between the distance from the bottom of the chamber (abscissa) and the temperature (ordinate) in Schaefer's continuous cloud chamber. Fig. 4 is a similar representation for the temperature distribution in the thermostat-type cloud chamber used in the present experiments. The upper curve shows the temperature distribution when the lower half of the chamber was maintained at −5C; the middle and lower curves indicate temperatures of −10 and −15C, respectively. These curves show only a slight variation of temperature (±0.1 ~ 0.2C) to a distance of 10 cm from the bottom of the chamber in marked contrast to the considerable temperature gradient of Schaefer's cloud chamber.

In making a run, the apparatus was first cooled to about −20C by refrigeration and the thermoregulator,

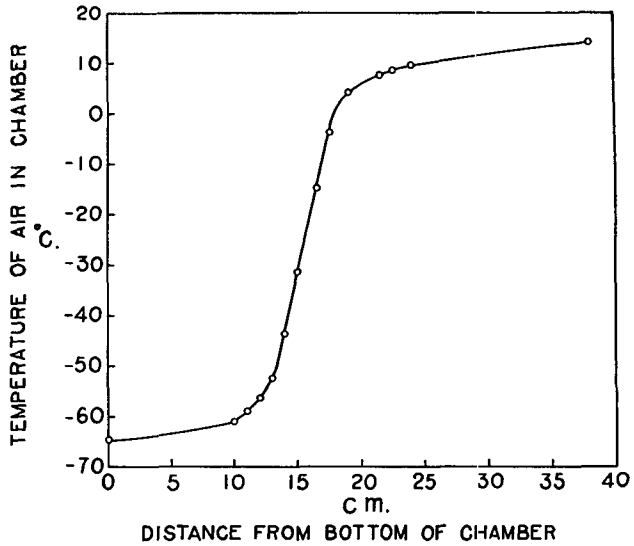

FIG. 3. Temperature profile in Schaefer's continuous cloud chamber.

water vapor was supplied from the generator and a fog of low concentration without a temperature gradient was formed in the chamber below the 10 cm level. Smoke made by the condensation or dispersion method was, after the test of its concentration through the ultra-microscopic method, diluted with clean air to a concentration of about 10^4 particles per cc, 10^5

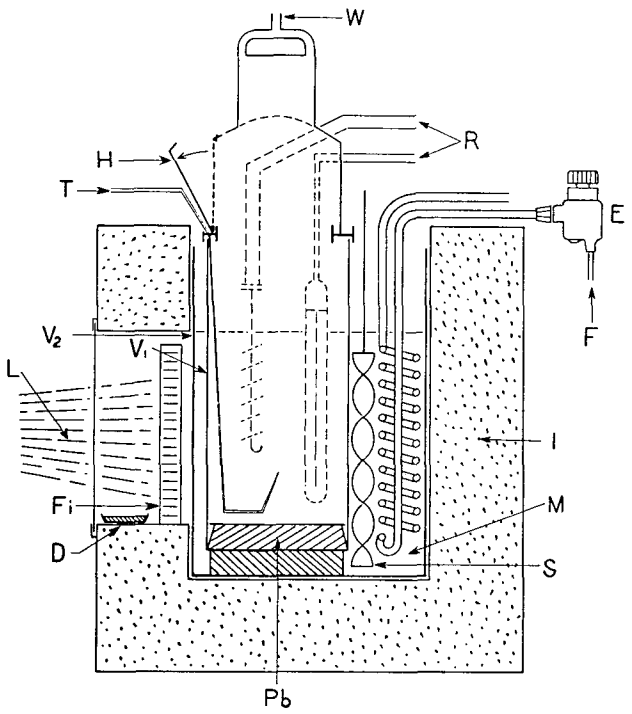

FIG. 2. Schematic drawing of thermostat-type cloud chamber. D: drying agent (P_2O_5), E: expansior, F: fleon, Fi: filter ($CuCl_2$ solution, 5 per cent), H: hinged glass-window, I: insulated box, L: light beam from 300 watt lamp, M: cooling medium ($CaCl_2$ solution, 25 per cent), Pb: lead block, R: thermoregulator, S: stirrer, T: copper-constantan thermocouple, V_1 and V_2: glass vessel, W: water vapor inlet.

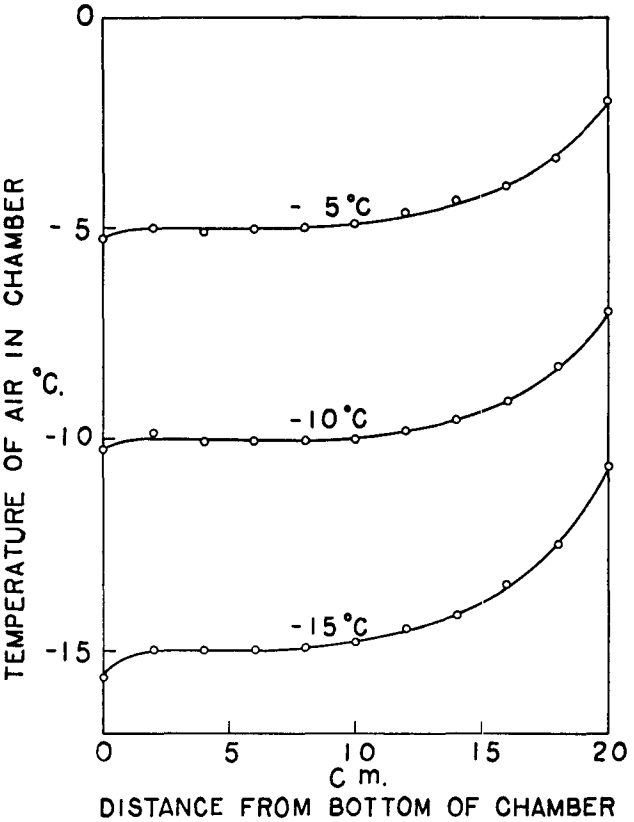

FIG. 4. Temperature distribution in author's thermostat-type cloud chamber.

particles of the aerosol were introduced by a syringe into the chamber through the hinged glass window (H) at the upper side of the glass vessel. Then a light beam (L) from which the heat rays above 6000 A were filtered by means of a five per cent aqueous cupric chloride solution [15; 16] was focused into the chamber and the number of ice crystals, growing and falling, in the first two minutes after addition of the aerosol was individually counted. Phosphorus pentoxide (D) was placed near the filter in order to prevent frost formation on the surface of the glass plates. Further runs were made at higher temperatures until the number of ice crystals falling for two minutes was just equal to 0.1 per cent of the aerosol particles. At the temperature, the velocity of ice-crystal formation was rather slower and ice crystals once formed fell out of sight in a few seconds. It was possible to find the temperature without fear of counting the same crystal more than once. In fact, for the range of 0.2 ~0.4C above the temperature the ice-crystal formation happened scarcely in most cases. When this critical temperature was thus determined by successive runs, the experiments were repeated in a like manner from higher temperatures to the critical one. In this way the threshold temperatures of various chemicals could be precisely determined.

3. Experimental results and discussion

The results of these experiments with regard to 80 varieties of chemicals of simple composition are shown in table 1; some of these, not only of hexagonal or cubic structure, but also water-soluble substances, were mentioned in our preliminary report [17]. The threshold temperatures are accurate to within ±0.2C for temperatures higher than −10C and ±0.4C for lower temperatures. The crystal systems, the crystal structures and the lattice constants are taken from Wyckoff [18]. For the compounds that have more than one crystal system and crystal structure at ordinary temperatures, the physical states considered probable from appearance, *e.g.* color, are listed.

It is obvious that lead iodide particles are the most active (−1.3C) of all substances tested in this experiment. Hosler observed ice crystals at temperatures as high as −4C with the nuclei; Schaefer [19] found that they were effective as sublimation nuclei at temperatures colder than about −5C; Mossop reported activity up to −7C and according to Birstein they were effective as ice nuclei at −20C. Vonnegut first pointed out that the crystal lattice of lead iodide matched the ice dimension even better than silver iodide along the *a*-axis; nevertheless, few investigators have noticed its remarkable ice-forming ability and it has long been considered less effective than silver iodide. The supposed ineffectiveness of lead iodide has been explained on the grounds that it has a much higher solubility in water than silver iodide. Despite this, the present results show that lead iodide is more effective as an ice nucleus than silver iodide. This fact seems to imply that the difference of solubilities cannot be a governing factor.

Bismuth iodide has a threshold temperature at −2.5C next to lead iodide, and it was found to be active as an ice crystal nucleus by Sano [9].

As has been observed by previous workers, we find that silver iodide can be active as ice nucleus at −2.6C. Vonnegut noted its ability as an ice nucleus and pointed out its structural similarity to ice crystals, and since then, it was observed to be the most active by Cwilong (−2.9 ± 0.1C) [20], Hosler (−3C), aufm Kampe (−3C), Sano (−6C), Birstein (higher than −20C) and so on.

As for silver bromide and silver chloride particles, prepared very carefully so as not to be contaminated by iodide ions, we find that these salts have threshold temperatures at −4.1 and −4.2C, respectively. No previous workers have examined these substances except Hosler who tested silver bromide and found it active in freezing supercooled clouds.

It was found that cupric and cuprous oxides also serve as ice nuclei at −4.3 and −4.5C, respectively, although Sano and his coworkers reported that cupric oxide was inactive. In view of these activities, it is expected that the copper compounds will be used in future field experiments because they are inexpensive and stable in comparison to silver iodide which is inactivated by irradiation with light [21; 22; 23; 24].

While mercurous iodide can cause ice crystal formation at temperatures up to −4.6C, it is decomposed by irradiation with light or by heating as follows [12; 25]

$$Hg_2I_2 \rightarrow Hg + HgI_2.$$

Both nickel and cobaltous oxides serve as ice-forming nuclei at −4.9C, but cobaltic oxide is inactive down to −17.9C.

The oxides of silver and nickel were shown to be effective at −5.2 and −6.1C each. Sano observed no ice-crystal formation with the former but the latter agrees with his result (−7C).

The temperatures of cadmium fluoride and aluminium oxide are nearly equal and are −6.4 and −6.5C, respectively. The latter was found to be an effective artificial nucleus as good as silver iodide by Asada and to be effective at −12C by Sano.

The author finds that silver sulfide causes nucleation of ice formation at −6.7C. However, the threshold temperature of −4C given by Hosler is to some extent higher than the author's. Birstein tested the same nucleus generated in nitrogen gas and reported it to be active at −20C.

TABLE 1. Threshold temperature, method of dispersal (c.: condensation method, d.: dispersion method) and crystal structure (C.: cubic, H.: hexagonal, H.Ps.: pseudo-hexagonal, M.: monoclinic, O.: orthorhombic, Rh.: rhombohedral, T.: tetragonal) of various chemical substances.

Compound	Threshold temperature (C)	Dispersion method	Crystal system	Crystal structure	Lattice constant a (A)	b (A)	c (A)
Ice			H.		4.5135		7.3521
PbI_2	− 1.3	c.	H.	$Cd(OH)_2$	4.54		6.86
BiI_3	− 2.5	c. & d.	Rh.		8.13		
			H.Ps.		7.498		20.68
AgI	− 2.6	c.	H.	ZnO	4.58		7.494
SnI_2	− 3.8	d.					
AgBr	− 4.1	c.	C.	NaCl	5.768		
AgCl	− 4.2	c.	C.	NaCl	5.547		
CuO	− 4.3	d.	M.		4.653	3.410	5.108
Cu_2O	− 4.5	d.	C.	Cu_2O	4.252		
Hg_2I_2*	− 4.6	d.	T.		4.92		11.61
NiF_2	− 4.9	d.	T.	SnO_2	4.710		3.118
CoO	− 4.9	d.	C.	NaCl	4.24		
Ag_2O	− 5.2	d.	C.	Cu_2O	4.72		
NiO	− 6.1	d.	C.	NaCl	4.1684		
CdF_2	− 6.4	d.	C.	CaF_2	5.40		
Al_2O_3	− 6.5	d.	C.		7.73–8.06		
Ag_2S	− 6.7	d.	M.		4.20	6.93	9.50
CeF_3	− 6.8	d.	H.	CeF_3	7.114		7.273
FeF_2*	− 7.0	d.	T.	SnO_2	4.670		3.297
Cu_2I_2	− 7.0	d.	C.	ZnS	6.0427		
CuS	− 7.3	d.	H.		3.80		16.43
PbF_2	− 7.5	d.	C.	CaF_2	5.942		
			O.		7.61	6.41	3.80
MgF_2	− 7.9	d.	T.	SnO_2	4.66		3.08
ZnF_2	− 7.9	d.	T.	SnO_2	4.715		3.13
CuF_2	− 8.1	d.	C.	CaF_2	5.406		
CaF_2	− 8.3	d.	C.	CaF_2	5.451		
Cu_2Cl_2	− 8.4	d.	C.	ZnS	5.4057		
LiF	− 8.5	d.	C.	NaCl	4.0173		
MgO	− 9.3	c.	C.	NaCl	4.203		
PbS	− 9.3	d.	C.	NaCl	5.9233		
CoS	− 9.9	d.	H.	NiAs	3.367		5.160
Cu_2Br_2	−10.0	d.	C.	ZnS	5.6806		
BaF_2	−10.1	d.	C.	CaF_2	6.187		
NiS	−10.1	d.	H.	NiAs	3.42		5.30
			Rh.		5.655		
CdO	−10.2	d.	C.	NaCl	4.689		
$HgBr_2$	−10.6	c.	O.		4.624	12.445	6.798
PbO	−10.6	d.	O.		5.459	4.723	5.859
$NiBr_2$*	−11.1	c.	H.	$CdCl_2$	6.465		
CdI_2*	−11.7	c.	H.	$Cd(OH)_2$	4.48		6.96
HgI_2*	−12.0	c.	O.	(yellow)	4.674	13.76	7.32
			T.	(red)			
KI	−12.1	c.	C.	NaCl	7.052		
NH_4F	−12.1	c.	H.	ZnO	4.39		7.02
KCl	−12.2	c.	C.	NaCl	6.278		
KBr	−12.4	c.	C.	NaCl	6.586		
$PbBr_2$	−12.5	c.	O.		9.518	8.038	4.717
MnO_2	−12.5	d.	T.	SnO_2	4.44		2.89
$MgBr_2$*	−12.7	c.	H.	$Cd(OH)_2$	3.81		6.26
NH_4I*	−12.8	c.	C.	NaCl	7.244		
$CdCl_2$	−12.8	c.	H.	$CdCl_2$	6.23		
CaI_2*	−13.0	c.	H.	$Cd(OH)_2$	4.48		6.96
ZnO	−13.3	d.	H.	ZnO	3.2426		5.1948
LiCl	−13.7	c.	C.	NaCl	5.12		
KF	−13.7	c.	C.	NaCl	5.34		
NH_4Br	−13.7	c.	C.	CsCl	3.866		
CdS	−13.8	d.	H.	ZnO	4.131		6.691
Hg_2Br_2	−13.8	d.	T.		4.65		11.10
SnO_2	−13.8	d.	T.	SnO_2	4.72		3.16
NaCl	−14.0	c.	C.	NaCl	5.62869		
MgI_2*	−14.0	c.	H.	$Cd(OH)_2$	4.14		6.88
$HgCl_2$	−14.0	c.	O.		4.325	12.735	5.963
NaI	−14.1	c.	C.	NaCl	6.462		
ZnI_2*	−14.1	c.	H.	$Cd(OH)_2$	4.25		6.54
NaBr	−14.2	c.	C.	NaCl	5.96095		
SnO	−17.6	d.	T.		3.796		4.816
ZnS	−17.7	d.	C.	ZnS	5.412		
$PbCl_2$	−17.7	c.	O.		9.030	7.608	4.525
NaF	−18.5	c.	C.	NaCl	4.62		
KCN*	−19.9	c.	C.	NaCl	6.51		
Hg_2Cl_2	−17.7>	c.	T.		4.47		10.89

* Considered to be partially decomposed.

TABLE 1—*Continued.*

Compound	Threshold temperature (C)	Dispersion method	Crystal system	Crystal structure	Lattice constant a (A)	b (A)	c (A)
HgS	−17.7>	d.	C.	ZnS	5.84		
TiO_2	−17.7>	d.	T.	SnO_2	4.4923		2.8930
SnS_2	−17.7>	d.	H.	$Cd(OH)_2$	3.639		5.868
HgO	−17.8>	d.	O.		3.296	3.513	5.504
$SnCl_2$	−17.8>	c.	O.		6.61	9.34	9.98
SnS	−17.8>	d.	O.		4.33	11.18	3.98
PbO_2	−17.8>	d.	T.	SnO_2	4.931		3.367
Co_2O_3	−17.9>	d.					
FeI_2*	−20.0>	c.	H.	$Cd(OH)_2$	4.04		6.75
MgTe*	−20.0>	d.	H.	ZnO	4.52		7.33
NH_4Cl	−22.0>	c.	C.	CsCl	4.047		

Using cuprous iodide Hosler observed ice crystals to form at −9C and this agrees fairly well with the author's value of −7C. The result obtained by Birstein shows the same tendency. That is, the nucleus generated in nitrogen is inactive as a nucleating agent though active when heated in air.

Cupric sulfide is effective at a relatively low temperature (−7.3C), though below that temperature it can very rapidly change a supercooled water cloud into ice crystals acting similarly to silver iodide or lead iodide at higher temperatures.

Lithium fluoride, reported inactive by Hosler and Birstein, was, on the contrary, observed to be effective in nucleation for ice formation at −7.3C. Though the present data do not agree with those of previous reports, the discrepancy may be due to the use of different sized particles. In any case, the present author made sure that particles of sufficient size were used since it has been pointed out that the threshold temperature is a function of particle diameter [1; 9] or, in other words, the larger the nucleus, the higher its threshold temperature.

Regarding magnesium oxide smoke generated by burning magnesium ribbon, we obtained a threshold temperature of −9.3C which is in accord with the result of Sano (−10C). Asada also showed that magnesium oxide smoke could become the nucleus of an ice crystal at temperatures below −13C, while Mossop observed ice formation with the nucleus at −28C.

For cadmium iodide, the threshold temperature of −9.5C given by d'Albe agrees well with present observations (−12C). The results of Hosler (−15C), Sano (−18C) and Birstein (−20C, on a smoke generated in air) are different from the author's. Birstein and Anderson state in their report that iodine has a positive ice-nucleating ability at −20C, and they propose as an explanation that whereas some iodides are found to be inactive when they were prepared as smoke by heating in nitrogen, they became active if prepared in air. According to them, these iodides yield iodine through the following reaction:

$$NH_4I \xrightarrow{\text{heat}} NH_3 + HI, \quad HI \longrightarrow \tfrac{1}{2}H_2 + \tfrac{1}{2}I_2$$
$$CdI_2 + \tfrac{1}{2}O_2 \longrightarrow CdO + I_2$$

when heated in air, and once iodine is produced, it may react further with minute traces of unknowns to form ice nuclei. The experimental results of Sano, however, indicate that iodine gives no ice-crystal formation until a temperature as low as −35C, is reached. The same result has been obtained in the author's qualitative test at −13C. Therefore, the activity of cadmium iodide may not be explained by the activity of iodine alone but ought to be explained by that of cadmium oxide or more probably of cadmium iodide itself. The author believes the latter two to be active from the present measurement although cadmium iodide was found to have poor ice-forming ability by Birstein and Anderson.

The threshold temperature for mercuric iodide smoke was reported to be −14C by Sano, −17C by Mossop and −18C by Hosler. The author's result, −12C, is the highest of all. It is well-known that the compound has its transition point at 126C and above that temperature the yellow orthorhombic type is stable; however, judging from the color of the smoke produced, the particles maybe have the red tetragonal structure which is stable at room temperature or below.

According to Hosler [7], highly polarizable ions and molecules, such as Ag^+, Pb^{++}, I^-, I_2 and O_3, might play a role in altering the surface structure of small drops. On entering the surface of droplets, they lower the surface free energy and this lowering of energy might permit the small droplets to change into ice crystals. Weyl [26], in line with this, alluded to the conception that the presence of highly polarizable ions weakens the distorting influence of the electrical double layer so that the atomic structure of the water droplets tends toward that of the normal arrangement and crystallization becomes possible.

Birstein made tests later on the same nuclei and proved that silver nitrate, ammonium iodide and ozone, prepared in nitrogen, were not effective at −20C; Sano and the author have confirmed Birstein's tests on the ineffectiveness of iodine, as mentioned above. It becomes clear from these experiments that no water-soluble salt has its threshold temperature higher than −11C. Especially, cadmium iodide, ammonium fluoride and calcium iodide belong in the hexagonal crystal systems and their lattice constants along the a-axis, 4.48, 4.39 and 4.48 A, respectively, are similar to the ice-crystal dimension, 4.5135 A. In spite of this, these compounds are not as effective as expected because of their high solubilities in water. The theory of Hosler [7] cited above concerning the action of polarizable ions reducing the surface free energy of droplets may not be in accordance with the phenomenon observed in this laboratory that all the soluble salts tested are not effective as ice nuclei at temperatures higher than −11C [17]. A more complete explanation may be the following: the formation of an ice embryo by the water molecules on the surface of the nucleus is hindered by mutual interaction between these surface water molecules and the molecules of the nucleus itself. That is, the surface of the nucleus is distorted by diffusing water molecules on the one hand and the ice clusters growing on the surface are destroyed by the penetration of molecules of water soluble nucleus into the ice embryo on the other hand.

The striking structural resemblance of magnesium telluride to ice (MgTe: $a = 4.52$, $c = 7.33$ A; ice: $a = 4.5135$, $c = 7.3521$ A; both are wurtzite structure) has led to the expectation that this compound would be an active ice nucleus [8]. However, tests in this laboratory on magnesium telluride smoke prepared by the direct reaction of magnesium and tellurium in a hydrogen stream and generated by the dispersion method indicate that the anticipated activity does not occur at temperatures above −20C. Reference to the literature [12] shows that magnesium telluride is readily decomposed on wetting; therefore the nucleus is inactive.

It is evident that in general the results from this laboratory are to some extent higher than those of previous investigators. These discrepancies arise from the differences in the working principle of the cloud chamber used by the author and those employed by other workers. Almost all of the past experimental data were obtained by making use of Schaefer's or Wilson's cloud chamber. Although the thermostat-type cloud chamber was used in this experiment, few investigators have utilized it on the grounds that it is rather difficult to change the temperature continuously so that, heretofore in the use of the chamber, either scanty experimental data have been obtained or only a few experiments on ice-nucleating ability at a definite temperature have been performed. There are several factors to consider in a continuous cloud chamber. It has the considerable temperature gradient of 11.2C per cm; using lead and silver iodides (particle radius, 0.2 and 0.1 μ; refer to fig. 1), the sedimentation velocities of the particles may be calculated to 0.0041 and 0.0013 cm per sec, respectively by the Stokes-Cunningham relation. Further, it is generally known that a short time lapse is required for the added smoke particles to act as ice nuclei and for growth to occur to the extent that the ice crystals are large enough to be seen with the naked eye in the supercooled cloud. For instance, the rate of formation of ice crystals by lead iodide nuclei, observed by the author, is given in table 2. When smoke is introduced into the chamber held at a temperature slightly lower than the threshold temperature, one or two minutes must elapse before the condition prescribed for the determination of the threshold temperature is attained, namely, that the number of crystals falling over a two-minute period is equal to 0.1 per cent of the smoke particles added. Assuming the time to be 1.5 min, the distance of fall for this time is 0.37 and 0.12 cm respectively for lead and silver iodide and therefore, these nuclei may be measured $11.2 \times 0.37 = 4.1$ and $11.2 \times 0.12 = 1.3$C lower.

There is at least one defect in the Wilson cloud chamber. When the chamber is expanded, a turbulence occurs which is caused by the temperature difference between the wall and the inner cloud. In view of this, it is possible to miss the nuclei unless an immediate effect is exhibited.

In addition, according to Adams [27], the surfaces of smoke particles tend to be spoiled easily by certain oily matter floating in the air. We have taken full precautions to avoid these difficulties. Employing a zone in the lower half of the chamber where no temperature gradient exists and where the temperature is always maintained constant we were able to determine exactly the threshold temperatures of nuclei substances.

In table 1, it may be seen that nuclei that are effective at relatively high temperatures have fluorine,

TABLE 2. Rate of ice formation by lead iodide nuclei.

Temperature (deg C)	Time necessary to transform 0.1 per cent-particles of smoke into ice crystals (second)
−1.4	143
−1.6	79
−2.1	31
−2.6	21
−4.0	14

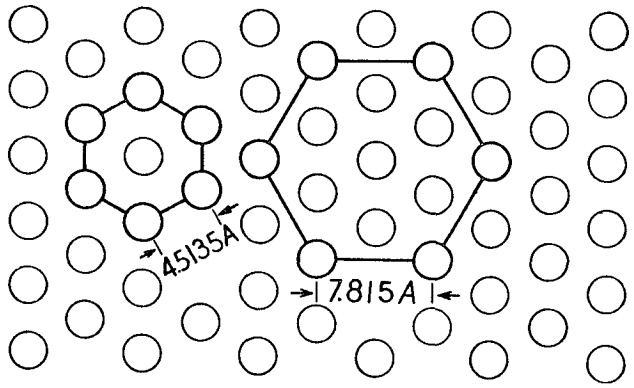

FIG. 5. The (0001)-plane of ice crystal. Circles denote positions of oxygen atoms.

iodine or oxygen as negative ions and silver or copper as positive ones. The activities of these substances in inducing crystallization are thought to be due to the interaction between the stronger electrostatic field of these ions constituting the surface of nuclei and that of the water dipoles. The substances mentioned here are all insoluble in water; this property is, as already stated, indispensable for activity as an ice nucleus.

The compounds of high threshold temperature are worthy of further comment. In table 1 the first (PbI_2) to the fourth (SnI_2) are all iodides and the most active, lead iodide, has a hexagonal cadmium hydroxide structure and a lattice plane (0001) which corresponds well with ice. The second, bismuth iodide, though rhombohedral, has a lattice constant of 7.498 A in the direction of a-axis assumed as hexagonal pseudo cell. This value is nearly equal to the length of one side of smallest sexangle, $4.5135 \times 3^{\frac{1}{2}} = 7.815$ A, which is obtainable by combining the oxygen atoms of ice outside the unit cell in the (0001) plane (refer to fig. 5; larger sexangle). Two crystal types, cubic and hexagonal, characterize the structure of silver iodide at ordinary temperatures; however, according to Manson's X-ray diffraction study [28], silver iodide has a hexagonal wurtzite structure when the smoke of this compound is generated by strong heating as in these studies. Both the a- and c-axes of silver iodide are very similar to those of ice. The crystal structure of the fourth, stannous iodide, remains as yet unknown and a reference to the literature [12] shows us that it crystallizes into orange-red octahedra. Therefore, the atomic distance and the bond angle of stannous iodide, obtained for its vapor by electron diffraction method, are given in comparison with that of lead iodide as follows [29];

$$\text{Sn} - \text{I} = 2.73\ \text{A}, \quad \text{I} - \text{Sn} - \text{I} = 95°$$
$$\text{Pb} - \text{I} = 2.79\ \text{A}.$$

These values are close to the distance of the neighboring oxygen atoms in ice, 2.76 A. From the chemical and structural similarity of stannous iodide to that of lead iodide one would expect the crystalline structure to resemble ice; further investigation is necessary on this point.

The nucleation process may be explained as follows: when water molecules are adsorbed on these nuclei, the free energy of the system is accordingly lowered, and in this state, the forming ice embryo requires a smaller amount of free energy for the reason that the atoms of the nucleus surface are of the same arrangement as the ice crystals. Consequently, the probability of nucleation is increased and ice formation can occur.

4. Conclusion

The results of the present experiments, free from the experimental errors generally overlooked up to now, indicate that: A. no water-soluble salts are effective as ice-forming nuclei at temperatures higher than −11C; B. stable and water insoluble compounds whose structures are similar to ice crystals are highly effective as ice nuclei; and C. the stronger the ionic nature of nucleus crystal, the more active the particle, if satisfying these two conditions.

From this evidence, it may be concluded that the role of the ice-forming nucleus in the atmospheric phase transition is at first the decrease of interfacial free energy by adsorption and a subsequent lowering of the free energy of embryo formation as a consequence of the structural similarity of the nucleus to the ice crystal. Water-insolubility is essential for effectiveness as a nucleus. Weyl's and Hosler's explanations and Facy's concept of eutectic mixtures [30] seem to be insufficient at least as far as the activity of a highly effective ice nucleus is concerned.

Acknowledgments.—The author wishes to express his thanks to Professor I. Sano for his many stimulating discussions and suggestions pertaining to the phenomena of ice nucleation. He is also deeply indebted to the financial support extended for this work by the Chūbu Electric Power Co., Ltd., Nagoya.

REFERENCES

1. Vonnegut, B., 1947: The nucleation of ice formation by silver iodide. *J. appl. Phys.*, **18**, 593–595.
2. Cwilong, B. M., 1947: Sublimation in a Wilson chamber. *Proc. Soc. London*, A, **190**, 137–143.
3. Fournier d'Albe, E. M., 1949: Some experiments on the condensation of water vapor at temperature below 0C. *Quart. J. r. meteor. Soc.*, **75**, 1–14.
4. Mossop, S. C., 1956: Sublimation nuclei. *Proc. phys. Soc.*, B, **69**, 161–164.
5. Mossop, S. C., 1956: The nucleation of supercooled water by various chemicals. *Proc. phys. Soc.*, B, **69**, 165–174.
6. Schaefer, V. J., 1952: Continuous cloud chamber for studying small particles in the atmosphere. *Ind. and Eng. Chem.*, **44**, 1381–1383.

7. Hosler, C. L., 1951: On the crystallization of supercooled clouds. *J. Meteor.*, **8**, 326–331.
8. Asada, T., H. Saito, T. Sawai, and S. Matsumoto, 1954: *Some experiments of artificial rain-making.* Report of rain-making in Japan, Vol. 1, 81–96.
9. Sano, I., Y. Fujitani, and Y. Maena, 1956: An experimental investigation on ice-nucleating properties of some chemical substances. *J. meteor. Soc. Japan*, **34**, 104–110.
10. aufm Kampe, H. J., and H. K. Weickmann, 1951: The effectiveness of natural and artificial aerosols as freezing nuclei. *J. Meteor.*, **8**, 283–288.
11. Birstein, S. J., and C. E. Anderson, 1955: The mechanism of atmospheric ice formation, I: the chemical composition of nucleating agents. *J. Meteor.*, **12**, 68–73.
12. Friend, J. N.: *Textbook of Inorganic Chemistry.* Charles Griffin & Co., London.
13. Brauer, G., 1954: *Handbuch der präparativen anorganischen Chemie.*
14. Schaefer, V. J., *Final Report, ONR Project*, G. E. Res. Lab., 1953, Dec., p. 61.
15. Nichols, 1893: *Phys. Rev.*, **1**, 13.
16. Coblenz, 1911: *Bur. Standards Bull.*, **7**, 655.
17. Sano, I., and N. Fukuta, 1956: Observations of the ice nucleating temperature of some chemical substances. *J. meteor. Soc. Japan*, **34**, 59–61.
18. Wyckoff, R. W. G., 1948: *Crystal structures*, Vol. 1.
19. Schaefer, V. J., 1954: Silver and lead iodides as ice-crystal nuclei. *J. Meteor.*, **11**, 417–419.
20. Cwilong, B. M., 1949: Sublimation in outdoor air and seeded sublimation. *Nature*, **163**, 727–728.
21. Inn, E. C. Y., 1951: Photolytic inactivation of ice forming silver iodide nuclei. *Bull. Amer. meteor. Soc.*, **32**, 132–135.
22. Reynolds, S. E., and W. Hume II, B. Vonnegut, and V. J. Schaefer, 1951: Effect of sunlight on the action of silver iodide particles as sublimation nuclei. *Bull. Amer. meteor. Soc.*, **32**, 47.
23. Reynolds, S. E., W. Hume II, and M. McWhirter, 1952: Effects of sunlight and ammonia on the action of silver iodide particles as sublimation nuclei. *Bull. Amer. meteor. Soc.*, **33**, 26–31.
24. Sano, I., and N. Fukuta, 1956: Effects of water vapor, ammonia and hydrogen sulfide against the decay of silver iodide smoke under irradiation of ultraviolet light. *J. meteor. Soc. Japan*, **34**, 34–40.
25. Mellor, J. W.: *Comprehensive treatise on Inorg. and Theoret. Chem.* Longmans, Green & Co., London.
26. Weyl, W. A., 1951: Surface structure of water and some of its physical and chemical manifestations. *J. Colloid Sci.*, **6**, 389–405.
27. Adams, N. K., 1949: *Phys. and Chem. of Surf.*, p. 174, Oxford.
28. Manson, J. E., 1954: An x-ray diffraction study of silver iodide aerosols. *J. appl. Phys.*, **26**, 423–425.
29. Lister, M. W., and L. E. Sutton, 1941: The investigation by electron diffraction of some dihalides of cadmium, tin and lead. *Trans. Farad. Soc.*, **37**, 406–419.
30. Facy, L., 1950: Lex noyaux artificiels de congelation. *J. sci. Météor.*, **2**, 7–18.